Journal of Biomolecular NMR, **26:** 69–77, 2003.
KLUWER/ESCOM

Backbone resonance assignment in large protonated proteins using a combination of new 3D TROSY-HN(CA)HA, 4D TROSY-HACANH and ^{13}C-detected HACACO experiments

Kaifeng Hu, Alexander Eletsky and Konstantin Pervushin*
Laboratorium für Physikalische Chemie, Eidgenössische Technische Hochschule Hönggerberg, CH-8093 Zürich, Switzerland

Received 8 January 2003; Accepted 30 January 2003

Key words: backbone resonance assignment, large proteins, multiple quantum, transverse relaxation optimization

Abstract

A new method for backbone resonance assignment suitable for large proteins with the natural ^{1}H isotope content is proposed based on a combination of the most sensitive TROSY-type triple-resonance experiments. These techniques include TROSY-HNCO, ^{13}C′-detected 3D multiple-quantum HACACO and the newly developed 3D TROSY multiple-quantum-HN(CA)HA and 4D TROSY multiple-quantum-HACANH experiments. The favorable relaxation properties of the multiple-quantum coherences, signal detection using the ^{13}C′ antiphase coherences, and the use of TROSY optimize the performance of the proposed set of experiments for application to large protonated proteins. The method is demonstrated with the 44 kDa uniformly ^{15}N,^{13}C-labeled and fractionally (35%) deuterated trimeric *B. Subtilis* Chorismate Mutase and is suitable for proteins with large correlation times but a relatively small number of residues, such as membrane proteins embedded in micelles or oligomeric proteins.

Abbreviations: TROSY – transverse relaxation-optimized spectroscopy; MQ – multiple quantum; nD – n-dimensional.

Introduction

In the recent years a method for the residue-specific assignment of the backbone resonances in large proteins has been developed, which is based on the implementation of transverse relaxation-optimized spectroscopy (TROSY) (Pervushin et al. 1997) in 3D and 4D sets of the triple-resonance experiments (Salzmann et al., 1999a, b; Yang and Kay, 1999; Mulder et al., 2000). The sensitivity of the basic TROSY-type HNCA, HNCOCA, HNCACB, HNCO and HNCACO experiments constituting this method is critically important for the successful backbone assignment. The uniform or partial replacement of non-labile protons with deuterons reducing transverse relaxation of the $^{1}H^{N}$ and $^{13}C^{\alpha,\beta}$ spins has been an indispensable tool for resolving and assigning NMR spectra of large complexes, including membrane proteins in detergent micelles (LeMaster, 1994; Yamazaki et al., 1994; Grzesiek et al., 1995b; Shan et al., 1996; Gardner and Kay, 1998; Salzmann et al., 1998). In this case much of the valuable side chain information is lost by the complete deuteration of these moieties. With the use of only partial deuteration the assignment process can be hampered by ^{13}C line broadening due to ^{1}H/^{2}H isotope effects (Venters et al., 1996). Other problems associated with the $^{1}H^{N}$ 'out-and-back' method underlying this line of experiments are the use of smaller scalar couplings $^{2}J_{NC_\alpha}$ (relative to $^{1}J_{NC_\alpha}$) to establish sequential correlations (Cavanagh et al., 1996), strong ^{13}C′ transverse relaxation due to the large ^{13}C′ CSA tensor, limiting the use of the HNCOCA-type experiments to spectrometers operating at lower po-

*To whom correspondence should be addressed. E-mail: kopeko@phys.chem.ethz.ch

larizing magnetic field strengths, and the need to back-exchange $^{2}H^{N}$ to protons.

Recently we proposed a new 3D multiple-quantum HACACO experiment (Eletsky and Pervushin, 2002) designed to complement this method. The use of the 3D MQ-HACACO experiment with proteins of larger molecular weight relies on the favorable relaxation properties of the $^{1}H^{\alpha}-^{13}C^{\alpha}$ multiple quantum coherences (Grzesiek et al., 1995a; Swapna et al., 1997; Xia et al., 2000) to record $^{1}H^{\alpha}$ and $^{13}C^{\alpha}$ chemical shifts and transfer the $^{1}H^{\alpha}$ magnetization to the $^{13}C'$ spins using one double constant-time evolution period (Swapna et al., 1997) and the direct acquisition of the $^{13}C'$ resonances (Serber et al., 2000, 2001). High sensitivity and a simple antiphase doublet structure of the $^{13}C'$ resonances enable effective signal acquisition even for large protonated proteins on the order of 50-60 kDa at room temperature. Sequential connectivities derived from weak sequential cross peaks in the 3D TROSY-HNCA experiments are complemented or completely replaced by strong one bond $^{13}C^{\alpha}$-$^{13}C'$ correlation cross-peaks obtained from the MQ-HACACO experiment, thereby 'bridging' intra-residual cross-peaks of the HNCA experiment with the strong inter-residual cross peaks derived from the HNCO experiment. Although 3D MQ-HACACO effectively resolves the problem of overlapping inter- and intra-residual $^{13}C^{\alpha}$ resonances (Salzmann et al., 1999b), bridging of the HNCA and HNCO experiments still relies on the consecutive matching of single pairs of the $^{13}C'$ (HNCO/HACACO) and $^{13}C^{\alpha}$ (HACACO/HNCA) chemical shifts. While good spectral resolution and large dispersion of the $^{13}C'$ chemical shifts facilitate the correlation between HNCO and HACACO experiments, broader lines along the $^{13}C^{\alpha}$ dimension in the 3D HACACO and 3D HNCA experiments might result in significant ambiguities in the assignment.

The remarkably good sensitivity obtained in the MQ-HACACO experiment (Eletsky and Pervushin, 2002) applied to large proteins with diluted ^{1}H isotope content encouraged us to explore the possibility of using $^{1}H^{\alpha}$ as well as $^{13}C^{\alpha}$ chemical shifts to reduce ambiguities in correlation of the backbone resonances. Here we describe two experiments, 3D multiple-quantum TROSY-HN(CA)HA, correlating the chemical shifts of the $^{1}H_{i}^{N}$, $^{15}N_{i}$ and intra-residual $^{1}H_{i}^{\alpha}$ spins, and 4D multiple-quantum TROSY-HACANH, correlating $^{1}H_{i}^{N}$, $^{15}N_{i}$, $^{13}C_{i}^{\alpha}$ and intra- residual $^{1}H_{i}^{\alpha}$ spins. Previously, enhancement factors of 1.5 to 1.7 were observed for 24 kDa ^{13}C, ^{15}N-labeled protein (FimC) when the standard triple-resonance schemes were upgraded to TROSY (Salzmann et al., 1998). We expect similar factors in our case.

Material and methods

BsCM is a water-soluble enzyme that catalyzes the rearrangement of chorismate to prephenate, a key step in the biosynthesis of the amino acids tyrosine and phenylalanine (Chook et al., 1994). It is a homotrimeric pseudo β-barrel surrounded by α-helices. Uniformly ^{15}N-, ^{13}C-, ^{2}H(35%)-labeled BsCM (DL-BsCM sample) and uniformly ^{15}N-, ^{13}C-, ^{2}H-labeled BsCM (TL-BsCM sample) were produced according to protocols described in (Eletsky et al., 2002) using Silantes CDN medium and Celtone medium, respectively. The protein concentration was 1 mM pro monomer dissolved in 25 mM potassium phosphate buffer at pH 7.5.

NMR experiments were performed at 293 K on a Bruker AVANCE 600 MHz spectrometer equipped with ^{13}C, ^{15}N, ^{1}H and ^{2}H tunable cryogenic probe. NMR data were processed with the program PROSA (Guntert et al., 1992). Chemical shifts are reported relative to DSS (sodium 2,2-dimethyl-2-silapentane-5-sulfonate).

Results and discussion

Figures 1a and 1b show the experimental schemes of 3D TROSY MQ-HN(CA)HA and 4D TROSY MQ-HACANH, utilizing the 'out-and-back' and 'out-and-stay' methods, respectively (Cavanagh et al., 1996). The product operator description of the TROSY coherence transfer pathway in 3D TROSY MQ-HN(CA)HA is given by Equation 1.

$$
\begin{aligned}
&0.5(H_z^N + N_z) \rightarrow -N_y\left(\frac{E}{2} - H_z^N\right)\\
&\rightarrow -2N_xC_z^{\alpha}\left(\frac{E}{2} - N_z^N\right) \rightarrow 2C_y^{\alpha}N_z\left(\frac{E}{2} - H_z^N\right)\\
&\rightarrow 4C_x^{\alpha}H_z^{\alpha}N_z\left(\frac{E}{2} - H_z^N\right)\\
&\rightarrow -4C_x^{\alpha}H_y^{\alpha}N_z\left(\frac{E}{2} - H_z^N\right)[t_2] \qquad (1)\\
&\rightarrow 2C_y^{\alpha}N_z\left(\frac{E}{2} - H_z^N\right)\\
&\rightarrow -2N_{\pm}C_z^{\alpha}\left(\frac{E}{2} - H_z^N\right)[t_1]\\
&\rightarrow H_-^N\left(\frac{E}{2} + N_z\right)[t_3],
\end{aligned}
$$

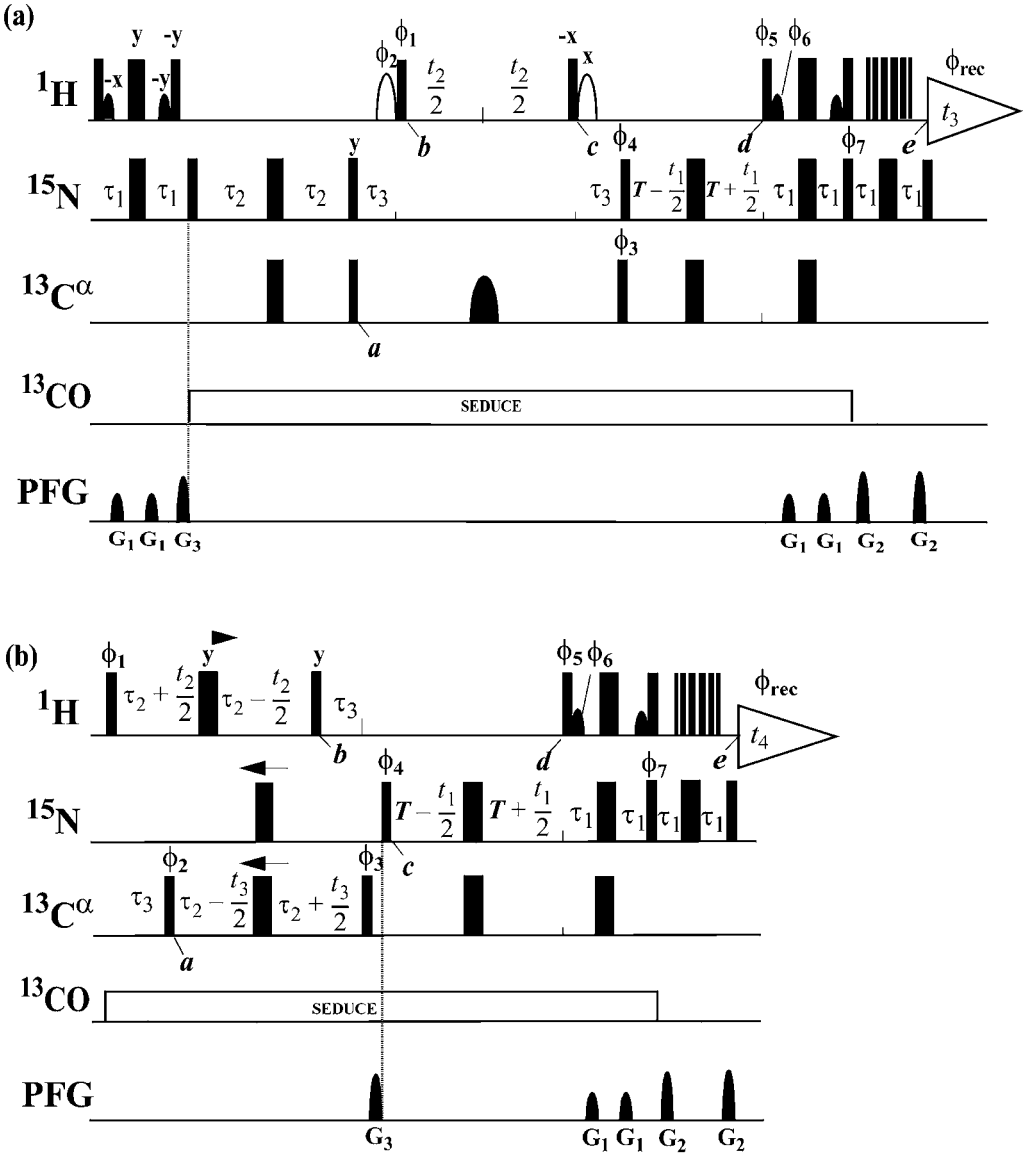

Figure 1. Experimental scheme for (a) 3D TROSY MQ-HN(CA)HA and (b) 4D TROSY MQ-HACANH experiment. The radio-frequency pulses on ^{1}H, ^{13}C$^\alpha$, ^{15}N and ^{13}C′ are applied at 4.7, 54.6, 119 and 173.6 ppm, respectively. Narrow and wide black bars indicate high power 90° and 180° pulses. Filled sine bell shapes on the line marked ^{1}H indicate water-selective 1 ms Gaussian 90° pulses applied to align the water magnetization in +z direction before data acquisition (Grzesiek and Bax, 1993). The residual transverse water magnetization is dephased using 3-9-19 composite pulses (Liu et al., 1998). Selective ^{13}C′ decoupling is achieved by SEDUCE-1 (Shaka et al., 1983) at a field strength of $\gamma B_2 = 1.65$ kHz. The line marked PFG indicates the duration and strength of pulsed magnetic field gradients applied along the z-axis: G_1: 0.9 ms, 40 G/cm; G_2: 1 ms, 80 G/cm; G_3: 0.5 ms, 50 G/cm and G_4: 0.9 ms, 40 G/cm. In (a) open shapes on the line marked ^{1}H indicate the ^{1}H^N band-selective 1.5 ms excitation E-Burp2 pulse (Geen and Freeman, 1991) with $\gamma B_1 = 2.73$ kHz with the phase ϕ_2 (time point b) and the time-reversed excitation E-Burp2 pulse with the phase x (time point c). The center of excitation for the ^{1}H^N band-selective pulses is placed at 9 ppm, so that all amide protons resonating between 11.5 and 6.5 ppm are returned to the +z axis. A filled sine bell shape on the line marked ^{13}C$^\alpha$ indicate 1.6 ms refocussing 180° Re-Burp pulse (Geen and Freeman, 1991) with $\gamma B_1 = 3.91$ kHz. The delays are $T = 14$ ms, $\tau_1 = 2.7$ ms, $\tau_2 = 14$ ms, $\tau_3 = 3.5$ ms. The phase cycle is: $\phi_1 = \{x\}$, $\phi_2 = \{-x\}$, $\phi_3 = \{4(-x), 4x\}$, $\phi_4 = \{y, -y, -x, x\}$; $\phi_5 = \{-y\}$; $\phi_6 = \{y\}$; $\phi_7 = \{-y\}$; $\phi_{rec} = \{y, -y, -x, x, -y, y, x, -x\}$. A phase-sensitive spectrum in the ^{15}N(t_1) dimension is obtained by recording a second FID for each t_1 value, with $\phi_4 = \{y, -y, x, -x\}$, $\phi_5 = \{y\}$, $\phi_6 = \{-y\}$ and $\phi_7 = \{y\}$. Quadrature detection in the ^{1}H (t_2) dimension is achieved by the States-TPPI method (Marion et al., 1989) applied simultaneously to the phases ϕ_1 and ϕ_2. In (b) the delays are $T = 14$ ms, $\tau_1 = 2.7$ ms, $\tau_2 = 12$ ms and $\tau_3 = 3.5$ ms. The phase cycle is: $\phi_1 = \{x\}$, $\phi_2 = \{x\}$, $\phi_3 = \{4x, 4(-x)\}$, $\phi_4 = \{y, -y, -x, x\}$; $\phi_5 = \{-y\}$; $\phi_6 = \{y\}$; $\phi_7 = \{-y\}$; $\phi_{rec} = \{y, -y, -x, x, -y, y, x, -x\}$. A phase-sensitive spectrum in the ^{15}N(t_1) dimension is obtained by recording a second FID for each t_1 value, with $\phi_4 = \{y, -y, x, -x\}$, $\phi_5 = \{y\}$, $\phi_6 = \{-y\}$ and $\phi_7 = \{y\}$. Quadrature detection in the ^{1}H (t_2) and ^{13}C^a(t_3) dimensions is achieved by the States-TPPI method (Marion et al., 1989) applied to the phases ϕ_1 and ϕ_2, respectively.

where H, N and C represent product operators of ^{1}H, ^{15}N and $^{13}C^{\alpha}$ spins, respectively. Single transition operators $H_-^N\left(\frac{E}{2}+N_z\right)$ and $N_\pm\left(\frac{E}{2}-H_z^N\right)$ represent slowly relaxing TROSY components of the ^{15}N-$^1H^N$ multiplet (Pervushin et al., 1997). The experimental scheme of Figure 1a deviates from the corresponding TROSY-HNCA experiment (Salzmann et al., 1998) at time point **a**, where the polarization transfer period τ_3 is inserted, resulting in the development of the $^{13}C^{\alpha}$ coherence antiphase relative to the directly attached $^1H^{\alpha}$ spin. This coherence is subsequently converted by the pulse ϕ_1 to the $^{13}C^{\alpha}$-$^1H^{\alpha}$ multiple quantum operator with favorable relaxation properties, used to record the $^1H^{\alpha}$ chemical shift. The high-power 90° ^{1}H excitation pulses applied at time points **b** and **c** are bracketed by $^1H^N$ band-selective 90° E-Burp2 pulses (Geen and Freeman, 1991), in order to preserve the spin state of the $^1H^N$ spins and to prevent exchange between TROSY and anti-TROSY ^{15}N multiplet components. In the middle of t_2 $^{13}C^{\alpha}$ chemical shift is refocussed by a 180° $^{13}C^{\alpha}$ band-selective Re-Burp pulse (Geen and Freeman, 1991), reducing signal attenuation due to the evolution of ^{13}C homonuclear passive J-couplings between $^{13}C^{\alpha}$ and $^{13}C^{\beta}$. The standard ST2-PT element (time points **d** and **e**) (Pervushin et al., 1998) is used to correlate the frequency of the TROSY component of the ^{15}N multiplet with the corresponding component of the $^1H^N$ multiplet.

Figure 1b shows the 4D TROSY MQ-HACANH experiment, based on the $^{13}C^{\alpha}$-$^1H^{\alpha}$ HMQC double constant-time magnetization transfer scheme and TROSY detection of the ^{15}N and $^1H^N$ chemical shifts. The product operator description of the relevant coherence transfer pathways is given by Equation 2.

$$\begin{aligned} H_z^{\alpha} &\rightarrow 2H_x^{\alpha}C_z^{\alpha} \rightarrow -2H_x^{\alpha}C_y^{\alpha}[t_2,t_3] \rightarrow 2C_y^{\alpha}N_z \\ &\rightarrow -2C_z^{\alpha}N_{\pm}\left(\frac{E}{2}-H_z^N\right)[t_1] \\ &\rightarrow H_-^N\left(\frac{E}{2}+N_z\right)[t_4]. \end{aligned} \tag{2}$$

The experimental scheme of Figure 1b is best suited for the methine C^{α} carbons, since full use of the double constant-time period can be made for the $^1H^{\alpha}$ and $^{13}C^{\alpha}$ chemical shift evolution. A modification of the experimental scheme of Figure 1b is required in order to detect with optimal sensitivity the methylene C^{α} carbons which occur in glycine residues. This version of the HACANH corresponds to the first part of the (HA)CA(CO)NH experiment introduced by (Swapna et al., 1997) and will not be described in detail in this paper. After the double-constant-time period $2\tau_2$, the resulting signal is determined by magnetization transfer from the $^1H^{\alpha}$ to $^{13}C^{\alpha}$ and subsequently to ^{15}N spins, as well as attenuation due to passive homonuclear J-couplings of $^1H^{\alpha}$ to $^1H^{\beta}$, $^1H^N$ spins and $^{13}C^{\alpha}$ to $^{13}C^{\beta}$ spins. Neglecting effects of relaxation and small heteronuclear J-couplings between $^1H^{\alpha}$ and $^{13}C^{\beta}$ and $^{13}C^{\alpha}$ and $^1H^{\beta}$ spins, the HMQC part of the transfer function is given by Equation 3:

$$\begin{aligned} I(\tau_2,\tau_3) &= \sin(\pi J_{H_i^{\alpha}C_i^{\alpha}}\tau_3)^2 \sin(2\pi J_{C_i^{\alpha}N_i}\tau_2) \\ &\cos(2\pi J_{H_i^{\alpha}H_i^N}\tau_2)\cos(2\pi J_{H_i^{\alpha}H_i^{\beta}}\tau_2) \\ &\cos(2\pi J_{C_i^{\alpha}N_{i-1}}\tau_2)\cos(2\pi J_{C_i^{\alpha}C_i^{\beta}}\tau_2). \end{aligned} \tag{3}$$

Transfer efficiencies of 0.28 and 0.21 are obtained for the α-helical and β-sheet secondary structure elements of a protein at the optimal transfer delays (τ_3 = 3.4 ms and $2\tau_2$ = 27 ms), determined using $^3J(H^{\alpha}\text{-}H^N)$ = 4 Hz and 9 Hz for α-helix and β-sheet, respectively, (Wuthrich, 1986) and $^3J(H^{\alpha}\text{-}H^{\beta 2}) \sim 12$ Hz, $^1J(C^{\alpha}\text{-}C^{\beta}) \sim 37$ Hz, $J(C^{\alpha}\text{-}N_i) \sim 9$ Hz and $J(C^{\alpha}\text{-}N_{i-1}) \sim 7$ Hz for both secondary structure elements (Cavanagh et al., 1996). In the experiment, a somewhat shorter delay ($2\tau_2$ = 24 ms) was used to compensate for the shift of the maximum of the function in Equation 3 due to transverse relaxation. Since the full delay can be used to record chemical shifts of $^1H^{\alpha}$ and $^{13}C^{\alpha}$ resonances, excellent resolution along the corresponding $^1H^{\alpha}$ and $^{13}C^{\alpha}$ dimensions can be obtained.

Sufficiently sensitive 3D TROSY MQ-HN(CA)HA, 3D TROSY MQ-HA(CA)NH and 4D TROSY MQ-HACANH spectra are obtained for the 44 kDa uniformly ^{15}N,^{13}C-labeled and fractionally 35% deuterated chorismate mutase from *Bacillus subtilis* (BsCM) (Eletsky et al., 2001) using the experimental schemes of Figure 1. Figure 2 compares the intensities of cross-peaks stemming from residues in the α-helical and β-sheet secondary structure elements of BsCM, obtained with the 3D TROSY MQ-HN(CA)HA and 3D TROSY MQ-HA(CA)NH experiments. Although sufficiently strong intra-residual $^1H^N$-$^1H^{\alpha}$ cross-peaks are identified in both experiments for most residues(see Figure 2), significantly different performance of these two experiments is observed for residues located in α-helices and β-sheets. Overall, higher sensitivity is detected for the α-helical regions of BsCM compared to the β-sheet or turn regions in the spectra measured with the 3D TROSY MQ-HA(CA)NH experiment (Figures 2b and 2d). Rather similar relative cross-peak amplitudes for α-helical and β-sheet are

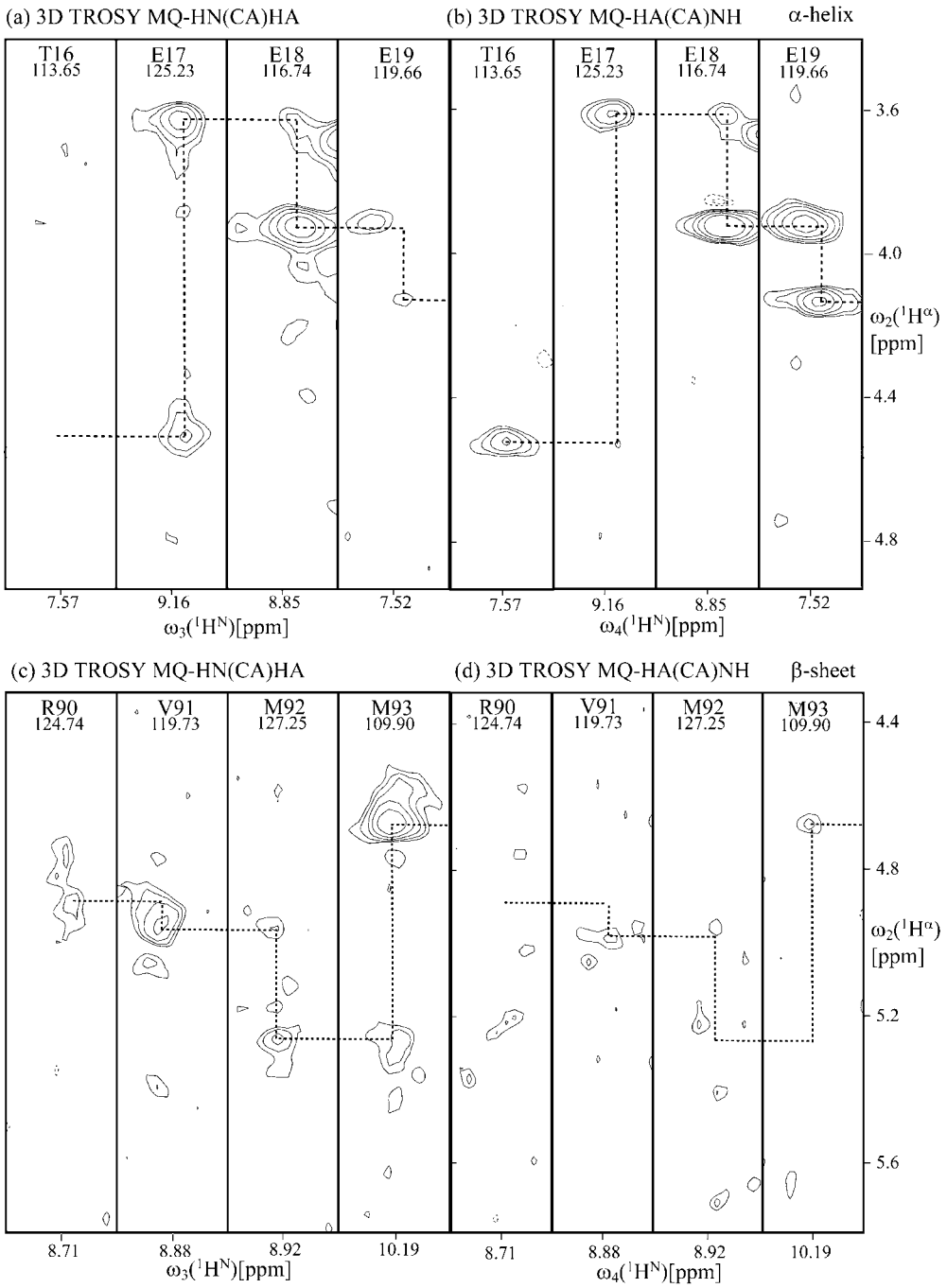

Figure 2. Comparison of corresponding 2D [$\omega_2(^1H^N)$, $\omega_{3/4}(^1H^N)$] strips from 3D TROSY MQ-HN(CA)HA (a and c) and 3D TROSY MQ-HA(CA)NH experiments (b and d) recorded with a 1 mM solution of the uniformly ^{15}N,^{13}C-labeled and fractionally 35% deuterated trimeric 44 kDa *B. Subtilis* Chorismate Mutase (BsCM). The strips were taken at the ^{15}N chemical shifts assigned to residues 16-19 and 90-93, located in the α-helical and β-sheet regions of BsCM, respectively. They are centered about the corresponding amide proton chemical shifts and have a width of 131 Hz along the $^1H^N$ dimension. The 4D TROSY MQ-HACANH experimental scheme of Figure 1b was acquired with $t_3 = 0$ resulting in the 3D TROSY MQ-HA(CA)NH experiment. For both experiments $40(t_1) \times 55(t_2) \times 512(t_3/t_4)$ complex points were accumulated, with $t_{1\max}(^{15}N) = 26.64$ ms, $t_{2\max}(^1H^\alpha) = 22.89$ ms and $t_{3/4\max}(^1H^N) = 53.25$ ms and 8 scans per increment resulting in a total measuring time of $\sim$ 22 h per spectrum. The sequential connectivities are indicated by dashed lines.

observed in spectra measured with the 3D TROSY MQ-HN(CA)HA experiment (Figures 2a and 2c). Although the average S/N over all residues of BsCM is slightly higher for MQ-HA(CA)NH than MQ-HN(CA)HA, the long double-constant-time period τ_2 renders the former experiment more sensitive to the deleterious effects of homonuclear passive *J*-couplings and transverse relaxation induced by dipole-dipole interactions of the $^1H^\alpha$ spins with remote proton spins. These factors result in a significant decrease of S/N in the β-sheet regions. Thus, for practical purposes the choice between the experimental schemes of Figure 1a and b can be determined by the predominance of a certain type of the secondary structure in the studied protein or both experiments can be tried for the best results.

The use of TROSY in the proposed experiments is justified by a direct comparison of signal-to-noise ratios in TROSY and conventional $^1H^N$-decoupled MQ-HA(CA)NH experiments. For all residues of ^{15}N-, ^{13}C-, ^2H(35%)-labeled 44 kDa BsCM the TROSY version exhibited S/N enhancement factors over the conventional implementation in the range of 1.1 to 1.5. These enhancement factors agree with to those previously observed for a 24 kDa ^{13}C,^{15}N-labeled protein (FimC) when the standard triple-resonance schemes were replaced with TROSY (Salzmann et al., 1998). It should be noted that for fully protonated large proteins smaller and non-uniform S/N enhancement factors in TROSY versions can be expected. This is attributed to the dominant contribution of the proton-proton spin-flip interactions to the TROSY ^{15}N relaxation rate (Kontaxis et al., 2000).

The presence of the $^{13}C^\alpha$-$^1H^\alpha$ HMQC double-constant-time period in the experimental scheme of Figure. 1b opens an attractive possibility of running TROSY MQ-HACANH in a 4D mode without compromising sensitivity of the experiment due to additional time incrementations, besides the loss in S/N due to the quadrature detection in the $^{13}C^\alpha$ dimension. Figure 3 illustrates the quality of the 4D spectrum measured using the 4D TROSY MQ-HACANH experiment with the 44 kDa uniformly ^{15}N,^{13}C-labeled and fractionally (35%) deuterated BsCM. Provided that sensitive sequential correlations are observed, the 4D TROSY MQ-HACANH experiment alone is sufficient to assign backbone resonances. In this experiment both $^1H^\alpha$ and $^{13}C^\alpha$ chemical shifts are used as reference for sequential connectivity assignment, which is less ambiguous and more reliable than only $^{13}C^\alpha$ chemical shift, as used in the conventional HNCA experiment. Figure 3 illustrates the process of sequential assignment obtained for a difficult case of Thr16, Glu17, Glu18 and Glu19 repeat.

Overall, the sole use of the 4D TROSY MQ-HACANH spectrum allowed establishing the sequential connectivities between 51 residues. The longest found continuous stretches of the connected residues are Thr16 to Glu34, Ala59 to Ser66, Trp68 to Val71 and Arg105 to Arg116. For the other residues either only intraresidual cross-peaks were found due to the lower intensity of the sequential cross-peaks (39 residues) or the corresponding strips were void of any cross-peaks (15 residues). For 20 residues the found connectivities were ambiguous. The use of the 3D HN(CA)HA in addition to the 4D TROSY MQ-HACANH spectrum helped to establish the sequential connectivities for Arg4, Ile6, Lys38 and His54.

The combined use of the 3D TROSY-HNCA, 3D TROSY-HNCO, 3D MQ-HACACO (Eletsky and Pervushin, 2002) experiments for residue specific assignment of the $^1H^\alpha$, $^1H^\nu$, ^{15}N, $^{13}C^\alpha$ and $^{13}C'$ backbone resonances is now effectively complemented by the 3D TROSY MQ-HN(CA)HA and 3D TROSY MQ-HA(CA)NH experiments. The 3D HA(CA)NH experiment is a reduced version of 4D HACANH of Figure 1. In this method sequential connectivities derived from weak sequential cross peaks in the 3D TROSY-HNCA experiments are replaced by strong one bond $^{13}C^\alpha$-$^{13}C'$ correlation cross-peaks obtained from the MQ-HACACO experiment. As shown in Figure 4, sequential correlations between protein backbone resonances can be obtained by matching the $^{13}C'$ chemical shifts in the HNCO/MQ-HACACO pair of experiments, obtained with sufficiently high resolution along the $^{13}C'$ dimension, with subsequent matching of the $^{13}C^\alpha$ and $^1H^\alpha$ chemical shifts in the MQ-HACACO/MQ-HACANH or MQ-HACACO/MQ-HN(CA)HA experiments.

The assignment process begins with the identification of the intraresidual and sequential $^{13}C^\alpha$ and $^{13}C'$ chemical shifts in HN strips taken from the TROSY-HNCA and TROSY-HNCO experiments, respectively. The intraresidiual $^1H^\alpha$ chemical shifts are identified using the 3D HA(CA)HN spectrum. If the 4D HACANH spectrum is available, the intraresidual $^1H^\alpha$ and $^{13}C^\alpha$ chemical shifts are found simultaneously and then $^{13}C^\alpha$ chemical shifts are verified using the TROSY-HNCA spectrum. At the next stage, connectivities between HN strips are established using 3D MQ-HACACO spectrum and verified for the cases where the sequential cross-peaks are resolved in

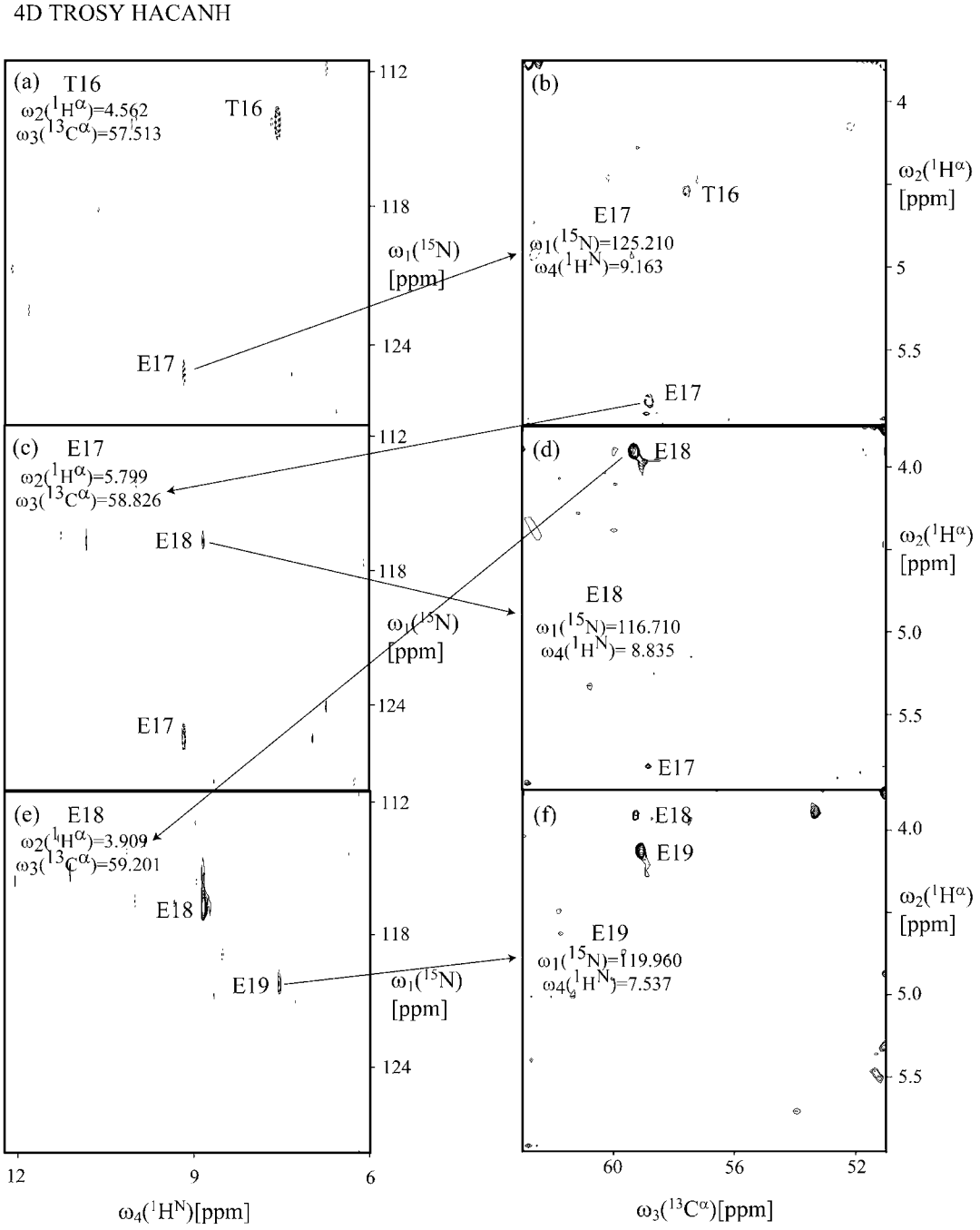

Figure 3. 2D [$\omega_1(^{15}N)$, $\omega_4(^1H^N)$] (a, c and e) and [$\omega_2(^1H^\alpha)$, $\omega_3(^{13}C^\alpha)$] (b, d and f) planes taken at the positions of the $^1H^\alpha$, $^{13}C^\alpha$ chemical shifts and the ^{15}N, $^1H^N$ chemical shifts, respectively, of residues 16-19 showing the procedure of sequential assignment of the backbone resonances using the 4D TROSY MQ-HACANH experiment of Figure 1b. 16 (t_1) × 30(t_2) × 40(t_3) × 512(t_4) complex points were accumulated, with $t_{1max}(^{15}N) = 10.65$ ms, $t_{2max}(^1H^\alpha) = 22.89$ ms, $t_{3max}(^{13}C^\alpha) = 22.21$ ms, $t_{4max}(^1H^N) = 53.25$ ms and 4 scans per increment resulting in the total measuring time of 5 days and 20 h. Sequential connectivities are indicated by arrows. In each 2D plane two chemical shifts of each residue associated with an individual cross-peak are indicated.

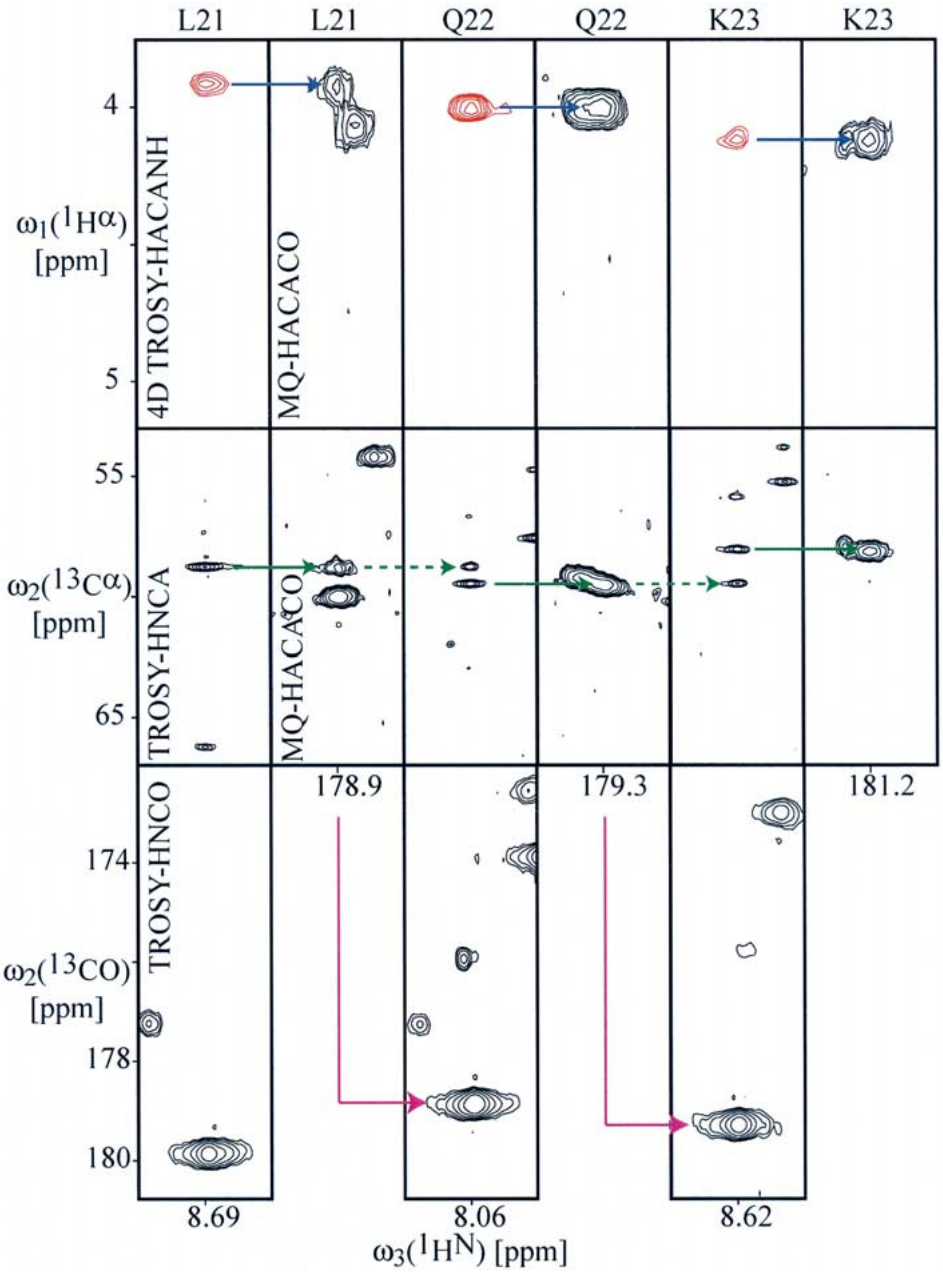

Figure 4. Method of assignment of the backbone $^{1}H^{\alpha}$, $^{13}C'$, $^{13}C^{\alpha}$ and ^{15}N resonance in uniformly ^{13}C, ^{15}N-labeled and fractionally deuterated large proteins using a combination of 3D TROSY-HNCA (Salzmann et al., 1998; Eletsky et al., 2001), 3D TROSY-HNCO (Salzmann et al., 1999b, c), 3D MQ-HACACO (Eletsky and Pervushin, 2002) and 4D HACANH experiments (shown in red) of Figure 1b. Arrows indicate a sequential walk through 2D $^{13}C^{\alpha}$-$^{1}H^{N}$, $^{13}C'$-$^{1}H^{N}$, $^{13}C^{\alpha}$-$^{13}C'$ and $^{1}H^{\alpha}$-$^{1}H^{N}$ strips taken at the positions of the corresponding ^{15}N, $^{13}C^{\alpha}$ and $^{1}H^{\alpha}$ resonances in 3D TROSY-HNCA, 3D TROSY-HNCO, 3D MQ-HACACO and 4D HACANH spectra, respectively. The assignment relies mostly on the connectivities shown by solid blue, green and magenta arrows. Occasionally the sequential connectivities of TROSY-HNCA, shown by dashed green arrows, are used.

TROSY-HNCA (see Figure 4). Thus connected HN strips are then mapped to the primary sequence of protein using the program MAPPER (Guntert et al., 2000). At this point it is very helpful to obtain the TROSY-HNCACB spectrum (Salzmann et al., 1999b) to reduce ambiguities in mapping. Thus, the minimal set of the triple-resonance experiments includes 3D TROSY-HNCA, 3D TROSY-HNCO performed with standard transfer delays (Cavanagh et al., 1996), 3D MQ-HACACO experiment and 3D HA(CA)NH experiment of Figure 1. If spectrometer time and sample stability permit, the 3D TROSY-HNCA and 3D HA(CA)NH experiments can be replaced by the single 4D HACANH experiment.

An attractive feature of this method is the requirement of only one fully protonated or partially deuterated protein sample to assign backbone resonances, which can be subsequently used for 3D structure determination. For proteins with large correlation times but a relatively small number of residues, such as membrane proteins embedded in micelles or oligomeric proteins this method alleviates the need to acquire the low sensitivity $^{13}C^{\alpha}$-constant-time TROSY-HNCA experiment (Salzmann et al., 1999a) and two or more of time-consuming 4D TROSY-type triple-resonance experiments (Konrat et al., 1999).

Acknowledgements

Financial support was obtained from the ETH Zürich internal grant to K.P. We thank Silantes AG for providing us with the ^{15}N-, ^{13}C- and $^{2}H(<35\%)$-labeled bacterial growth medium for the BsCM preparation. We thank Prof Donald Hilvert and Alexander Kienhöfer, ETH Zürich, for the preparation of the NMR samples of BsCM.

References

Cavanagh, J., Fairbrother, W.J., Palmer, A.G. and Skelton, N.J. (1996) *Protein NMR Spectroscopy: Principles and Practice*, Academic Press, New York.

Chook, Y.M., Gray, J.V., Ke, H.M. and Lipscomb, W.N. (1994) *J. Mol. Biol.*, **240**, 476–500.

Eletsky, A. and Pervushin, K. (2002) *J. Biomol. NMR*.

Eletsky, A., Heinz, T., Moreira, O., Kienhöfer, A., Hilvert, D. and Pervushin, K. (2002) *J. Biomol NMR*., **24**, 31–39.

Eletsky, A., Kienhöfer, A. and Pervushin, K. (2001) *J. Biomol. NMR*, **20**, 177–180.

Gardner, K.H. and Kay, L.E. (1998) *Annu. Rev. Biophys. Biomolec. Struct.*, **27**, 357–406.

Geen, H. and Freeman, R. (1991) *J. Magn. Reson.*, **93**, 93–141.

Grzesiek, S. and Bax, A. (1993) *J. Am. Chem. Soc.*, **115**, 12593–12594.

Grzesiek, S., Kuboniwa, H., Hinck, A. P. and Bax, A. (1995a) *J. Am. Chem. Soc.*, **117**, 5312– 5315.

Grzesiek, S., Wingfield, P., Stahl, S., Kaufman, J.D. and Bax, A. (1995b) *J. Am. Chem. Soc.*, **117**, 9594–9595.

Guntert, P., Dötsch, V., Wider, G. and Wüthrich, K. (1992) *J. Biomol. NMR*, **2**, 619–629.

Guntert, P., Salzmann, M., Braun, D. and Wüthrich, K. (2000) *J. Biomol. NMR*, **18**, 129–137.

Konrat, R., Yang, D.W. and Kay, L.E. (1999) *J. Biomol. NMR*, **15**, 309–313.

Kontaxis, G., Clore, G.M. and Bax, A. (2000) *J. Magn. Reson.*, **143**, 184–196.

LeMaster, D.M. (1994) *Prog. Nucl. Magn. Reson. Spectrosc.*, **26**, 371–419.

Liu, M.L., Mao, X.A., Ye, C.H., Huang, H., Nicholson, J.K. and Lindon, J.C. (1998) *J. Magn. Reson.*, **132**, 125–129.

Marion, D., Ikura, M., Tschudin, R. and Bax, A. (1989) *J. Magn. Reson.*, **85**, 393–399.

Mulder, F.A.A., Ayed, A., Yang, D.W., Arrowsmith, C.H. and Kay, L.E. (2000) *J. Biomol. NMR*, **18**, 173–176.

Pervushin, K., Riek, R., Wider, G. and Wüthrich, K. (1997) *Proc. Natl. Acad. Sci. U.S.A.*, **94**, 12366–12371.

Pervushin, K., Wider, G. and Wüthrich, K. (1998) *J. Biomol. NMR*, **12**, 345–348.

Salzmann, M., Pervushin, K., Wider, G., Senn, H. and Wüthrich, K. (1998) *Proc. Natl. Acad. Sci. USA*, **95**, 13585–13590.

Salzmann, M., Pervushin, K., Wider, G., Senn, H. and Wüthrich, K. (1999a) *J. Biomol. NMR*, **14**, 85–88.

Salzmann, M., Wider, G., Pervushin, K., Senn, H. and Wüthrich, K. (1999b) *J. Am. Chem. Soc.*, **121**, 844–848.

Salzmann, M., Wider, G., Pervushin, K. and Wüthrich, K. (1999c) *J. Biomol. NMR*, **15**, 181–184.

Serber, Z., Richter, C. and Dotsch, V. (2001) *Chembiochem*, **2**, 247–251.

Serber, Z., Richter, C., Moskau, D., Bohlen, J.M., Gerfin, T., Marek, D., Haberli, M., Baselgia, L., Laukien, F., Stern, A.S., Hoch, J.C. and Dotsch, V. (2000) *J. Am. Chem. Soc.*, **122**, 3554–3555.

Shaka, A.J., Keeler, J., Frenkiel, T. and Freeman, R. (1983) *J. Magn. Reson.*, **52**, 335–338.

Shan, X., Gardner, K.H., Muhandiram, D.R., Rao, N.S., Arrowsmith, C.H. and Kay, L.E. (1996) *J. Am. Chem. Soc.*, **118**, 6570–6579.

Swapna, G.V.T., Rios, C.B., Shang, Z.G. and Montelione, G.T. (1997) *J. Biomol. NMR*, **9**, 105–111.

Venters, R.A., Farmer, B.T., Fierke, C.A. and Spicer, L.D. (1996) *J. Mol. Biol.*, **264**, 1101–1116.

Wüthrich, K. (1986) *NMR of Proteins and Nucleic Acids*, Wiley, New York.

Xia, Y.L., Kong, X.M., Smith, D.K., Liu, Y., Man, D. and Zhu, G. (2000) *J. Magn. Reson.*, **143**, 407–410.

Yamazaki, T., Lee, W., Arrowsmith, C.H., Muhandiram, D.R. and Kay, L.E. (1994) *J. Am. Chem. Soc.*, **116**, 11655–11666.

Yang, D.W. and Kay, L.E. (1999) *J. Am. Chem. Soc.*, **121**, 2571–2575.